phys. stat. sol. (b) **245**, No. 9, 1858–1864 (2008) / **DOI** 10.1002/pssb.200879532

physica status solidi b
www.pss-b.com
basic solid state physics

Interatomic distances in pyrite-structure disulfides – a case for ellipsoidal modeling of sulfur ions

M. Birkholz[*,1] **and R. Rudert**[2]

[1] IHP, Im Technologiepark 25, 15236 Frankfurt (Oder), Germany
[2] Institute for Chemistry and Biochemistry of FU Berlin c/o BESSY, Albert-Einstein-Str. 15, 12489 Berlin, Germany

Received 31 January 2008, revised 4 June 2008, accepted 4 June 2008
Published online 23 July 2008

Dedicated to Prof. Helmut Tributsch on the occasion of his 65th birthday

PACS 61.50.–f, 61.50.Ah, 61.66.Fn

[*] Corresponding author: e-mail birkholz@ihp-microelectronics.com

The geometry of crystalline bonding in pyrite-structure disulfides MS_2 is investigated for the M = Mn, Fe, Co, Ni, Cu series. The decomposition of interatomic distances by the ionic radii approach is first shown to yield metal ion values r_M inconsistent with state-of-the-art data. The bonding geometry is subsequently analyzed by assuming sulfur ions to become ellipsoidally deformed in accordance with their crystallographic site symmetry. It is derived, how the S bonding coordination can be modeled by a polar radius $r_{\|}$ in direction of the trigonal axis and an equatorial radius $r_{\perp}$ perpendicular to it. Sulfur ions are found to compress along the symmetry axis yielding $r_{\perp}/r_{\|}$ ratios between 1.55 and 1.73 in the MnS_2–CuS_2 series and the additivity of the interatomic M–S distance from ion-specific parameters is re-established. A constant volume of $V_S = 0.0133$ nm^3 is consistently attained by sulfur ions in all MS_2 investigated. Finally, the crystal electric field acting at sulfur sites is uncovered to determine the ion deformation ratio $(r_{\perp} - r_{\|})/\sqrt[3]{3V_S/(4\pi)}$ with unexpected precision. These results imply that polarizable ions at polar lattice sites should appropriately be modeled by ellipsoids rather than by spheres.

1 Introduction The crystallographic structure of pyrite as taken by the name-giving chemical compound of composition FeS_2 was among the earliest structures solved by X-ray diffraction procedures. Already in 1914 William Lawrence Bragg derived from X-ray powder reflection patterns that the Fe ions build up a face-centered cubic lattice, into which the sulfur ions are embedded [1]. Herein, the latter reside on ⟨111⟩ diagonals and group in S_2 pairs or dumbbells. While the Fe ions are nearly octahedrally coordinated, the sulfur surrounding is that of a tetrahedron with 3Fe forming the basis and the neighbor S residing on top. The pyrite structure is related to that of fluorite, but while F ions in CaF_2 occupy the center positions (1/4 1/4 1/4) etc. within the eight subcubes of the Ca fcc lattice, sulfur ions in FeS_2 exhibit a further structural degree of freedom characterized by a positional parameter u that specifies their positions (*uuu*) etc. along ⟨111⟩ axes. The full site symmetry of Fe and S is accounted for by point group C_{3i} and C_3, respectively, while the primitive unit cell belongs to space group T_h^6 or $Pa\bar{3}$ (No. 205 according to *International Tables for Crystallography* [2]).

Since the early days of crystallography pyrite-type compounds became a fundamental testing ground of solid state physics due to their interesting structure-property relations [3, 4]. The prototype compound FeS_2 is a semiconductor and it was realized by Tributsch that semiconductors from the group of transition metal dichalcogenides should have the advantage of not essentially weakening chemical bonding on charge carrier generation [5]. In particular, the high absorption coefficient of pyrite FeS_2 for visible light offered promising perspectives for thin film photovoltaics [6–8]. For this application the introduction of few amounts of Fe-substituting Zn was favored in a theoretical study [9]. At the current state of knowledge, however, the decisive obstacle for a broad application of pyrite in large-area electronics seems to be related to the

sulfur deficiency that might be associated with the formation of defect bands in the forbidden zone [10–12]. Numerous applications of pyrite-structure dichalcogenides for energy storage [13], thermoelectrics, corrosion protections and other areas are intensively investigated at the moment. Of particular interest appears the role played by photoelectrochemical processes on pyrite surfaces in the prebiotic evolution on our planet [14, 15].

Although pyrite-type compounds belong to the group of most-intensively studied crystalline solids, the pyrite structure still hides a geometric secret that is related to its incompatibility with the concept of ionic radii. This geometrical modeling has successfully been used for the prediction of interatomic distances in crystalline solids mainly from the groups of halides and oxides [16, 17], but yields conflicting results of only little usefulness for sulfides and other heteropolar crystals. It has been proposed by Birkholz that these contradictions may be resolved, when the effects of crystal electric fields and ionic polarization are taken into account as they occur at polar lattice sites in heteropolar crystals [18]. Such a crystal electric field also arises on sulfur lattice sites of point group symmetry C_3 and its strength has first been determined in Ref. [19]. It leads to various interesting physical consequences like the polarization energy that has to be included into crystal energy considerations [19, 20] and a deformation of sulfur electronic orbitals, by which the high optical absorption coefficient of pyrite in a Stark effect like manner may be understood [21].

It will be investigated in this work whether the non-inversional site symmetry, to which sulfur ions are subjected in the pyrite lattice, is associated with a deviation of the ions shape from the form of a sphere. Within the framework of the presented model, sulfur ions in MS_2 will be regarded as deformable ellipsoids rather than rigid spheres. For this purpose, the geometrical shape of S ions will be described by a polar radius $r_{\parallel}$ and an equatorial radius $r_{\perp}$ directed along the $\langle 111 \rangle$ symmetry axis and perpendicular to it. It will be shown that the ellipsoidal deformation is governed by the strength of the crystal electrical field $\boldsymbol{E}_{\mathrm{CF}}$ active on sulfur lattice sites and that consistent sets of ionic volumes rather than ionic radii are obtained by application of the concept to different pyrite disulfides. Before presenting the derivations and results, the classical assumption of spherical ion shapes will be shown to result in metal ion radii r_{M} that are incompatible with state-of-the-art values as derived from the bond distance analysis of a large set of crystalline solids.

2 Failure of the concept of ionic radii The crystal radii of the sulfur and metal ions will now be determined by the conventional approach of decomposing the bond length between anions and cations, from which the crystal is composed of. For this purpose, only sulfur containing pyrite compounds MS_2 from 3d transition metals, M = Mn, Fe, Co, Ni and Cu, will be considered, because their structural parameters have been determined with high accuracy [22–26]. ZnS_2 will not be considered here, since structural parameters of the required precision are still missing to the best knowledge of the authors. The metal and sulfur ions will as usual be represented by formally divalent and monovalent ions M^{2+} and S^{-}. The radii obtained will be compared to the state-of-the-art values as given by Shannon and Prewitt [16] and Shannon [17], who analyzed a number of some hundred fluoride and oxide crystals and categorized the data according to the charge and spin state of ions and according to their coordination number and bonding geometry (abbreviated by SPS in the following).

Figure 1 shows a section along the (110) plane through the pyrite unit cell displaying the S_2 dumbbell at (*uuu*) and $(\bar{u}\,\bar{u}\,\bar{u})$ and the Fe ions at (1/2 1/2 0) and (1/2 1/2 1) from the first sulfur bonding spheres, while other Fe ions are omitted for clarity. The interatomic distances between metal-sulfur and sulfur–sulfur sites are denoted by d_{MS} and d_{SS} in the figure and depend on lattice constant a and sulfur positional parameter u through

$$d_{\mathrm{SS}} = a\sqrt{3}(1-2u)\,, \tag{1}$$

$$d_{\mathrm{MS}} = a\sqrt{2(1/2-u)^2+u^2}\,. \tag{2}$$

The two sulfur ions are modeled by spheres of radius r_{S} that touch at (1/2 1/2 1/2), from which it may be deduced that the sulfur ions exhibit an ionic radius of

$$r_{\mathrm{S}} = d_{\mathrm{SS}}/2 = a\sqrt{3}(1/2-u)\,. \tag{3}$$

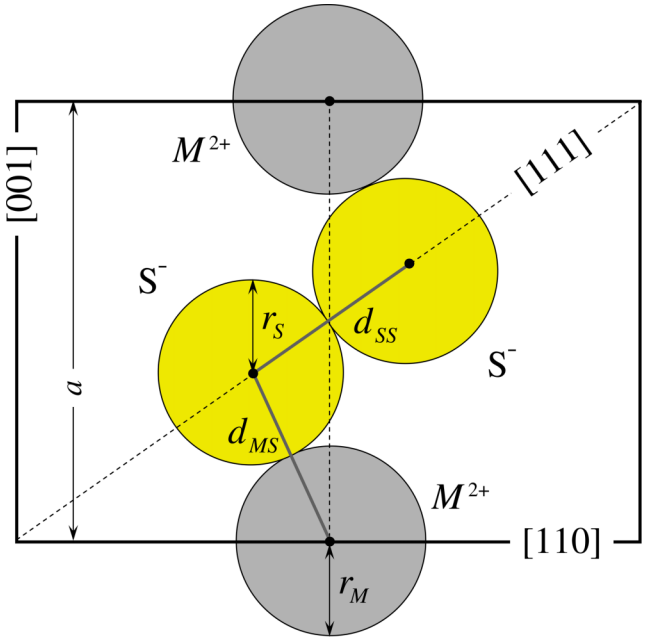

Figure 1 (online colour at: www.pss-b.com) (110) section through MS_2 pyrite unit cell with spherical representation of M^{2+} and S^{-} ions. Other metal ions than nearest neighbors of sulfur ions have been omitted.

Table 1 Structure parameters a and u of some pyrite-type sulfides MS_2 from cited references and derived quantities sulfur–sulfur and metal–sulfur bond lengths d_{SS} and d_{MS}, sulfur ionic radius r_S, metal ionic radius r_M according to Eq. (4), metal ionic radius according to SPS r_{MSP} [16, 17], relative difference δr_M between r_M and r_{MSP}.

MS_2	a (nm)	u	Ref.	d_{SS} (nm)	d_{MS} (nm)	r_S (nm)	r_M (nm)	r_{MSP} (nm)	δr_M
FeS_2	0.54160	0.38484	[22]	0.2161	0.2263	0.1080	0.1183	0.061	94%
CoS_2	0.55385	0.38987	[23]	0.2113	0.2325	0.1056	0.1269	0.065	95%
NiS_2	0.56852	0.39454	[24]	0.2077	0.2398	0.1038	0.1359	0.069	97%
CuS_2	0.57891	0.39878	[25]	0.2030	0.2453	0.1015	0.1438	0.073	97%
MnS_2	0.6104	0.4011	[26]	0.2091	0.2593	0.1046	0.1547	0.083	86%

From this result the ionic radii of the metal ions may be derived. In the firstly assumed model of rigid ion spheres to describe both the metal and the sulfur ions, the metal ion radius r_M simply becomes the difference between bond length and sulfur ionic radius

$$r_M = d_{MS} - r_S \,. \tag{4}$$

Values according to this straightforward approach have been determined for d_{MS}, d_{SS}, r_S and r_M for a set of sulfur-containing pyrite compounds and are given in Table 1. The sulfur radius r_S is seen from the table to attain a nearly constant value of 0.104 nm and to vary by only ±2% in the 3d MS_2 series. This value appears rather small, when compared to two-fold negatively charged S^{2-} ions exhibiting an ionic radius of 0.184 nm [16]. Although both ions S^- and S^{2-} differ by their net charge, the difference of about 80% appears implausible large to be caused by the addition of a single electron or – differently stated – the ionic radius of S^- as determined from the procedure applied above appears too small.

The conclusion is supported by the analysis of metal radii as calculated by application of Eq. (4) and given in the r_M column of Table 1. In order to compare these results to state-of-the-art data, also the ionic radii r_{MSP} according to the comprehensive SPS listings are given in the table. For this purpose, r_{MSP} of divalent ions in an octahedral bonding geometry derived from oxide rather than halide crystals were selected, since the metal coordination in sulfides may be assumed to better compare to the first than to the latter (if differences occurred between Refs. [16] and [17], data from the later published work were preferred). Albeit this set of metal ionic radii r_{MSP} appear a reliable choice, large relative deviations $\delta r_M = (r_M - r_{MSP})/r_{MSP}$ on the order of 90% are obtained, when SPS values and those according to Eq. (4) are compared. The differences are so large that the modeling of ions by the geometric form of spheres in pyrite-structure disulfides appears doubtful in general. It must be concluded that the modeling of ions in the pyrite structure by rigid spheres yields incompatible results when compared with state-of-the-art ionic radii.

The discrepancy is usually regarded as an inadequacy of the rigid ion model and the metal-sulfur bond in pyrite disulfides is argued to exhibit a significant portion of covalency. As correct this statement appears in its generality, it offers no quantitative solution to deal with the inadequacy. In the following section it will be investigated whether the more general modeling of sulfur ions by ellipsoids rather than by spheres may solve the discrepancy and lead to consistent quantitative results.

3 Modeling of sulfur ions by ellipsoids It will be assumed in the following that a crystal electrical field is acting on the sulfur position causing a deformation of ions along the principal trigonal axis. The assumption is justified by a missing center of inversion at the sulfur lattice site allowing for a non-vanishing electrical field to occur that is caused by the (theoretically) infinite number of surrounding ions. Such a crystal electrical field $\boldsymbol{E}_{CF}$ only arises for sulfur ions, but vanishes at metal positions due to the different point group symmetries C_3 and C_{3i} of both lattice sites [19]. The crystal electrical field can be calculated with the help of a second-order Madelung constant β_j^m, where subscript j stands for the respective lattice site, being M or S here, and superscript m indicates the infinite sum to run over monopoles. $\boldsymbol{E}_{CF}$ then depends on β_j^m and the inverse square of the lattice constant a according to $\boldsymbol{E}_{CF} = e\beta_j^m/(4\pi\varepsilon_0 a^2)$, with e and ε_0 standing for the unit charge and the permittivity of vacuum. The electrostatic lattice constant β_j^m represents a second-order term in the general Taylor expansion of electrostatic interactions in a crystal lattice [20]. It only depends on the sulfur positional parameter u and the net charges of the ions, being +2 and −1 for M and S in the case considered here.

The geometrical constraints of the model, again, are displayed in a schematic section through the (110) plane, Fig. 2, but this time for the assumption of ellipsoidal shaped sulfur ions. The crystal electrical field $\boldsymbol{E}_{CF}$ at the sulfur position is always directed towards the dumbbell neighbor in accordance with the point group symmetry of the lattice site. Therefore, crystal electrical fields at (uuu) and ($\bar{u}\,\bar{u}\,\bar{u}$) are pointed towards each other as shown in the figure. However, no crystal electrical fields arise in the perpendicular direction. We thus have to distinguish between the geometrical extensions of the sulfur ion along two mutually perpendicular directions, which is appropriately modeled by a rotational ellipsoid, with its axis of rotation coinciding with the sulfur-sulfur bond. We are thus lead to distinguish between a polar radius $r_\parallel$ parallel to the axis of rotation and an equatorial radius $r_\perp$ perpendicular to

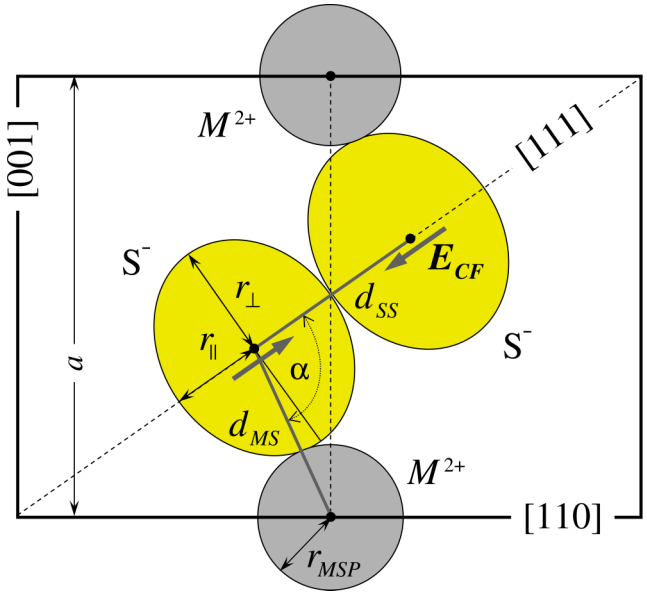

Figure 2 (online colour at: www.pss-b.com) (110) section through MS_2 pyrite unit cell with spherical representation of M^{2+} and ellipsoid modeling of S^- ions.

the latter. Such a geometric object is denoted mathematically correct as a spheroid, which is an ellipsoid with two major axes having the same length. Therefore, both expressions will be used interchangeably in the following. The volume of the S ion would then be given by

$$V_S = \frac{4\pi}{3} r_\perp^2 r_\parallel \,. \tag{5}$$

The geometrical quantities $r_\parallel$, $r_\perp$ and V_S will now be deduced. It is evident that the polar radius $r_\parallel$ simply derives from the sulfur-sulfur bond length as in Eq. (3)

$$r_\parallel = d_{SS}/2 = a\sqrt{3}(1/2 - u) \,. \tag{6}$$

However, the expression for $r_\perp$ is more complex and for its derivation, it has to be realized that its orientation deviates from the direction of the metal–sulfur bond. The difference may be quantified by introducing the angle between d_{SS} and d_{MS} denoted by α and given by

$$\cos\alpha = \frac{2 - 6u}{\sqrt{6(1 - 4u + 6u^2)}} \,. \tag{7}$$

The S–S–M bond angle α and other parameters like $r_\parallel$ etc. have been calculated and compiled in Table 2. It can be seen from the table that the S–S–M bond angle is smaller than the ideal tetrahedron angle of 109° for all listed compounds indicating the S bonding tetrahedron to be compressed along the direction of the sulfur–sulfur bond. By usage of the angle α, the M–S bond length may now be expressed as a function of the metal ion radius r_{MSP} and the parameters $r_\parallel$ and $r_\perp$ indicative of the sulfur ion volume

$$d_{MS} = r_{MSP} + \sqrt{r_\parallel^2 \cos^2\alpha + r_\perp^2 \sin^2\alpha} \,. \tag{8}$$

Table 2 S–S–M bond angle α and geometric S ion parameters in 3d transition metal pyrite sulfides. The polar and equatorial radii $r_\parallel$ and $r_\perp$, and their ratio, the S ion volume V_S and the sphere equivalent radius $\overline{r_S}$ were calculated for each compound according to Eqs. (6), (8), (5) and (9).

MS_2	α (°)	$r_\parallel$ (nm)	$r_\perp$ (nm)	$r_\perp/r_\parallel$	V_S (nm^3)	$\overline{r_S}$ (nm)
FeS_2	102.3	0.1079	0.1676	1.551	0.01271	0.1448
CoS_2	103.5	0.1056	0.1704	1.613	0.01285	0.1453
NiS_2	104.6	0.1038	0.1744	1.679	0.01323	0.1467
CuS_2	105.5	0.1015	0.1766	1.740	0.01325	0.1468
MnS_2	106.0	0.1047	0.1810	1.731	0.01434	0.1507
averages and standard deviations					0.0133 ±0.0006	0.1469 ±0.0021

It has to be emphasized that d_{MS} does not derive from the sum of the metal ion radius plus the equatorial radius $r_\perp$ of the sulfur spheroid, which would only hold for $\alpha = 90°$. For any S–S–M bond angle α different from 90° the full decomposition of the M–S bond length into three different parameters r_{MSP}, $r_\parallel$ and $r_\perp$ in accordance with Eq. (8) has to be performed. This, at a first sight, seemingly complicated composition of the M–S interatomic distance might have been the reason, why such separation has not been performed yet.

Equation (8) may only be solved by presupposing one radius, since there are three unknowns contained in only two Eqs. (6) and (8). One possible solution is obtained by inserting the SPS radii r_{MSP} for octahedrally coordinated and divalent M ions. This appears a reliable choice, because the metal ions occupy crystallographic lattice sites of inversional symmetry in the unit cell and are thus not subjected to a crystal electrical field and an induced deformation as are the sulfur ions ($\beta_M^m = 0$). Of course, also the symmetry of metal lattice site in the pyrite structure allows for electrostatic moments to occur, but those moments are of higher than dipolar order and are assumed to be negligible for the analysis performed here.

Table 2 presents the equatorial radii $r_\perp$ of S ion spheroids in the different pyrite-type disulfides. The values are seen to exceed the polar radii $r_\parallel$ in all cases by a factor of about 1.6. Sulfur ions in pyrite disulfides would accordingly have to be described by oblate ellipsoids, i.e. they become compressed along the polar axis and expand along the perpendicular direction. Also the sulfur ion volume V_S as calculated from Eq. (5) is listed in Table 2. These values show only a small scatter around an average ionic volume of $\overline{V_S} = 0.0133(6)$ nm^3 and a less than 5% standard deviation (given for the last digits in parentheses).

In order to compare the precision of these results with those from the conventional ionic radii approach, the sulfur ionic volume V_S may be transformed to an appropriate length scale. For this purpose, a sphere-equivalent radius of the sulfur ion is calculated from $r_\parallel$ and $r_\perp$ via

$$\overline{r_S} = \sqrt[3]{r_\perp^2 r_\parallel} \,. \tag{9}$$

Table 3 S ellipsoidal deformation ratio η, electrostatic lattice coefficient β_S^m and crystal electric field at S ion lattice site in units of β_S^m/a^2 for 3d transition metal pyrite sulfides.

MS_2	η	β_S^m	β_S^m/a^2 (nm^{-2})
FeS_2	0.411	5.244	17.88
CoS_2	0.446	5.954	19.41
NiS_2	0.481	6.683	20.68
CuS_2	0.511	7.414	22.12
MnS_2	0.507	7.847	21.06

This length gives the radius a spherical monovalent sulfur ion would have without the $\boldsymbol{E}_{CF}$-induced deformation. The mean sphere-equivalent radius as obtained by averaging over all compounds in the table yields $\overline{r}_S = 0.147(2)$ nm. This result compares much better to the ionic radius of divalent sulfur of 0.184 nm and the standard deviation of $\overline{r}_S$ amounts to only 1.5%. Moreover, the uncertainty δd_{MS} of interatomic M–S distances according to Eq. (8) also assumes only a small value of maximally 1.5%, since metal radii differences δr_M essentially vanish by selecting r_{MSP} values from the SPS data set. This is an excellent agreement when compared to the deviations δd_{MS} of about 90% as obtained by the ionic radius approach in the previous section. It can be concluded that the additivity of interatomic M–S distances from ion-specific length parameters is re-established by an ellipsoidal modeling of sulfur ions and a decomposition of d_{MS} in accordance with Eq. (8).

These results strongly suggest to consider the volume of monovalent sulfur ions V_S rather than its radius as a constant physical quantity – a statement, which seems to hold at least for the disulfides investigated here. In fact, this conclusion can be regarded as the generalization of the usual crystal radii approach, where, implicitly, also the ansatz of conserved ionic volume is made. But in the crystal radius concept both the volume and the radius are assumed constant in different crystals, and interatomic distances may then decompose into ion-specific radii. However, in the approach we are led to by the considerations given above, one of the assumptions has to be dropped and it may only be assumed that the sulfur ionic volume is conserved: while V_S remains constant, the deformation of ellipsoids will vary, i.e. the spheroidal radii $r_\parallel$ and $r_\perp$ will attain different values in different crystal surroundings. From the little variations of V_S or $\overline{r}_S$ given in Table 3, we may indeed conclude that this model correctly accounts for the geometry of bonding in pyrite-structure disulfides.

4 Discussion It has been argued so far that the crystal electrical field at the sulfur position causes a polarization and deformation of sulfur ions. The degree of deformation as given by the two ellipsoidal radii $r_\parallel$ and $r_\perp$ has been calculated for some S-containing compounds from their structural data by simple geometric considerations. The results obtained are so convincing that one may pose the question, whether the strength of the crystal electrical field $\boldsymbol{E}_{CF}$ could be correlated with the S ion deformation. In order to investigate this question quantitatively, the deformation ratio η will be introduced that is defined by

$$\eta = (r_\perp - r_\parallel)/\overline{r}_S \ . \tag{10}$$

This figure relates the ellipsoidal radii difference to the radius a sphere of the same volume would have and thus quantitatively describes the ellipsoidal deformation of the sulfur ion in the constant ionic volume approach. Values of the deformation ratio η have been determined for all MS_2 compounds and compiled in Table 3. They are seen to extend from 0.411 to 0.507.

It is interesting to note from Table 3 that the S ions in both CuS_2 and MnS_2 exhibit the largest ellipsoidal compression along the ⟨111⟩ axis as can be seen from the highest η values in excess of 0.5. In their case the polar radius $r_\parallel$ is maximally reduced at the expense of the equatorial one $r_\perp$ when compared with other 3d disulfides. It has been revealed experimentally that synthetic samples of CuS_2 and MnS_2 may only be prepared at elevated pressures in the 65 kbar range [25–28]. This contrasts remarkably with other disulfides FeS_2, CoS_2 and NiS_2 having smaller η values and lower S ion deformations, and which may be prepared under much lower pressure conditions in the laboratory. This means that the deformation ratio given by Eq. (10) has a direct physical meaning, i.e. the ellipsoidal deformation of S ions in the pyrite lattice translates into a mechanical load, to which the material must be subjected during preparation. The critical η value above which a mechanical stress has to be applied for the synthesis of 3d pyrite disulfides will be located in the 48 … 0.50 range. This unexpected correlation between a crystallographic quantity $(r_\perp - r_\parallel)/\overline{r}_S$ and thermodynamic preparation constrains underlines the significance and usefulness of decomposing the S ion volume in two orthogonal radii.

We will now come back to the question of a possible correlation between ion deformation and the strength of the crystal electric field. For this purpose, also second-order Madelung constants β_S^m are given in Table 3. The electrostatic lattice coefficients β_S^m are defined as the sum over electrical fields $\boldsymbol{E}_j$ caused by point charges z_i at crystal lattice sites $\rho_i = \boldsymbol{r}_i/a$. In case of the pyrite structure they are defined for the sulfur ion position through

$$\beta_S^m = \sum_i \frac{z_i}{\rho_i^3} \langle \boldsymbol{n} | \boldsymbol{\rho}_i \rangle \ , \tag{11}$$

where the projection upon unit vector $\boldsymbol{n}$ has to be taken along the symmetry axis, i.e. along ⟨111⟩ for S^- at (*uuu*). The β_S^m become dimensionless quantities, when defined in the form of Eq. (11). Numerical values for MS_2 pyrites investigated here have been determined by techniques as outlined in Refs. [19, 29]. The crystal electrical field $\boldsymbol{E}_{CF}$ is derived from β_S^m coefficient by multiplying with $e/(4\pi\varepsilon_0 a^2)$. In the following, for reasons of brevity only the ratio β_S^m/a^2 will be calculated for the determination of $\boldsymbol{E}_{CF}$.

According to Eq. (11), the β_S^m coefficient at the S lattice site becomes a function of sulfur positional parameter

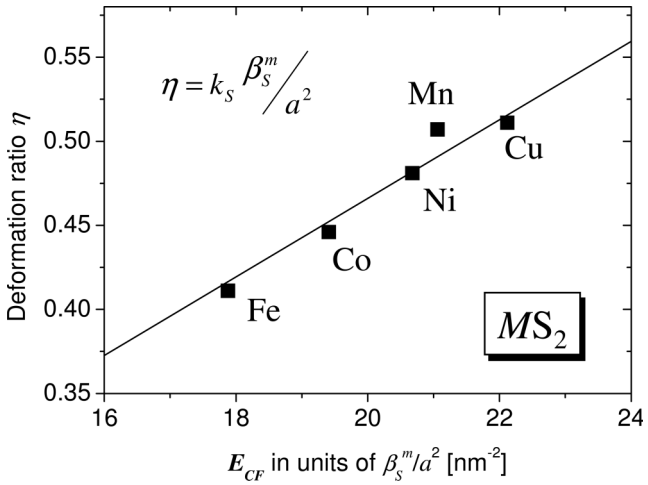

Figure 3 Deformation ratio η of pyrite structure disulfides versus crystal electric field $\boldsymbol{E}_{\mathrm{CF}}$ at sulfur lattice site (squares). The solid line gives a numerical fit according to Eq. (12).

u and it can be seen from Table 3 that it increases for increasing u. Although the β_{S}^m coefficients relate to the electrical field from all the surrounding ions, its increase with u is easily understood from a consideration of the interaction with the neighbor S ion alone: since increasing u accounts for lowering the interatomic distance d_{SS}, the Coulomb repulsion with the neighbor S^- increases, too, and thus leads to a further strengthening of the crystal electrical field.

Figure 3 displays the deformation ratio η for all pyrite compounds considered here versus the crystal electric field. A tendency of the data points for a continuous increase of η with increasing $\boldsymbol{E}_{\mathrm{CF}}$ can clearly be seen from the plot. This result is in agreement with our simple model, by which the sulfur ion would deviate the stronger from the shape of a sphere, the more intense the polarizing field becomes. The data points given in Fig. 3 were subjected to a numerical regression by using a linear test function

$$\eta = k_{\mathrm{S}}' E_{\mathrm{CF}} = k_{\mathrm{S}} \frac{\beta_{\mathrm{S}}^m}{a^2} \tag{12}$$

with constant k_{S} serving as fit parameter. The physical meaning of k_{S} is that of an ionic deformability that would usefully be assumed to attain the same value for a particular ion in a theory of chemical bonding in heteropolar crystals. Also the data pair $(\boldsymbol{E}_{\mathrm{CF}}, \eta) = (0, 0)$ was included into the regression, which accounts for a vanishing crystal electric field causing the ion spheroid to conserve a spherical shape ($\eta = 0$ or $r_\perp = r_\parallel$).

Figure 3 shows the course of the model function (12) as a solid line for $k_{\mathrm{S}} = 0.0234(5)$ nm^2. An excellent agreement between model function and experimental data points has to be stated, which is reflected by the small estimated standard deviation of 2.1% of the proportionality constant k_{S}. The error bars of experimental data points are of the size of their symbols and are mainly caused by the standard deviations of r_{MSP} values, which were assumed to be on the order of their last numerical digit specified in the SPS tables [16, 17].

The remarkable agreement between the model function and experimental data points displayed in Fig. 3 comes as a surprise because of the following argument. As can be seen from Eq. (11), the values of $\boldsymbol{E}_{\mathrm{CF}}$ as calculated from β_{S}^m coefficients give the strength of the crystal electric field at the center positions (*uuu*) of sulfur ions. However, the sulfur ion is a spatially extended charge distribution that interacts with the spatially extended crystal electrical field $\boldsymbol{E}_{\mathrm{CF}}(xyz)$. Any correlation between deformation ratio η and $\boldsymbol{E}_{\mathrm{CF}}(uuu)$ can thus only be an approximation, by which the β_{S}^m/a^2 value serves as an average of the full crystal electric field $\boldsymbol{E}_{\mathrm{CF}}(xyz)$. In view of this implicitly included approximation, the tendency of η data points to follow the course of $\boldsymbol{E}_{\mathrm{CF}}$ is unexpectedly well pronounced. We think that this clear correlation might be understood by the fact that sulfur ions in all disulfides investigated here are subjected to nearly the same crystal electric field distribution, since they all occupy the same symmetry sites in a pyrite-structure unit cell. Therefore, $\boldsymbol{E}_{\mathrm{CF}}$ values indicated by β_{S}^m/a^2 seem to represent a very reasonable average. Assuming this argument being valid, the ionic deformability k_S would not only depend on the ion under consideration, but also on the crystalline surrounding.

The strongest deviation from the model function (12) is realized to occur for the data point of MnS_2. The Mn^{2+} ion has been identified to exhibit a high-spin d^5 configuration in MnS_2 [26, 30] being associated with an occupation of e_g and t_{2g} states by five unpaired electrons [28]. This contrasts to the other members of the MS_2 series, where metal e_g and t_{2g} states are successively filled by progressing from FeS_2 to CuS_2 [28]. In part, the effect has been taken into account by selecting the metal ionic radius for Mn^{2+} in the high-spin configuration given in the SPS tables [16, 17]. But in view of the arguments outlined in the previous paragraph, it might be conjectured that the averaging of the crystal electric field distribution $\boldsymbol{E}_{\mathrm{CF}}(xyz)$ in high-spin MnS_2 is distinct from that in the low-spin members of MS_2 disulfides. This reasoning might justify to omit the MnS_2 data point for the numerical regression altogether, resulting in a fitting constant of 0.0231(2) nm^2 with a furthermore reduced estimated standard deviation.

It also has to be mentioned that the correct valency of Cu and the S_2 dumbbell in CuS_2 is controversially discussed. While it has been argued in favor of divalent Cu from the increase of interatomic distances d_{MS} along the line from FeS_2 to CuS_2 [25], experimental evidence has been given that the charge configuration is $3d^{10}$ and the Cu ion thus is in a predominantly monovalent state [31]. In accordance with this study, the complete sulfur dumbbell is frequently assumed to attain a formal charge of -1. The surplus electron would then spread over the full S_2 unit and a single sulfur ion would only inappropriately be modeled by a S^- charge assignment in CuS_2.

We think that the solution of the last points mentioned deserves further theoretical considerations and studies us-

ing the approach presented in this work. Irrespective of these critical remarks and their prospective investigations, it has to be stated that an excellent agreement between experimental data and the course of the model function (12) has been obtained. The crystal electric field can indeed be concluded to determine the sulfur ion deformation.

5 Conclusions We are thus led to a consistent geometrical model of crystalline bonding in 3d transition metal pyrite disulfides: while the sulfur ion attains a constant volume V_S in all compounds, its spatial extension along the trigonal axis and perpendicular to it must be described by distinct radii $r_\parallel$ and $r_\perp$. Accordingly, the shape of the sulfur ion has to be modeled by an ellipsoid rather than a sphere. The geometrical analysis yields a sulfur ionic volume of $V_S = 0.0133$ nm^3. This quantity has the character of a crystal-chemical constant and can be expected to be generally attained by monovalent sulfur ions in heteropolar crystals.

The S ion deformation in disulfides from the MnS_2–CuS_2 series studied in this work is that of an oblate spheroid with a compression along the trigonal axis. The amount of ion deformation is distinct in different MS_2 and has been quantified by the deformation ratio $\eta = (r_\perp - r_\parallel)/\sqrt[3]{3V_S/(4\pi)}$. It turned out that the strength of the deformation is governed by the crystal electric field present at the sulfur lattice site and can be described by a deformability parameter k_S and a second-order electrostatic lattice constant β_S^m. The structural parameters – being them either lattice constant a and positional parameter u or, equivalently, the interatomic distances d_{SS} and d_{MS} – of pyrite-structure disulfides then finally become an unambiguous function of the ion-specific constants r_{MSP}, V_S and k_S. The modeling of sulfur ions by ellipsoids rather than by spheres yielded very reasonable results with respect to the prediction of interatomic distances.

Acknowledgement We gratefully acknowledge Jarek Dabrowski for critical reading and discussion of the manuscript.

References

[1] W. L. Bragg, Proc. R. Soc. Lond. **89**, 468 (1914).
[2] T. Hahn (ed.), International Tables for X-ray Crystallography, Vol. A (Kluwer Academic Publishers, Dordrecht, 2002).
[3] D. J. Vaughan and J. R. Craig, Mineral chemistry of metal sulfides (Cambridge University Press, Cambridge, 1978).
[4] K. Sato, Progr. Cryst. Growth Charact. **11**, 104 (1985).
[5] H. Tributsch, Z. Naturforsch. **32A**, 972 (1977).
[6] G. Smestad, A. Da Silva, H. Tributsch, S. Fiechter, M. Kunst, N. Meziani, and M. Birkholz, Sol. Energy Mater. **18**, 299 (1989).
[7] A. Ennaoui, S. Fiechter, C. Pettenkofer, N. Alonso-Vante, K. Büker, M. Bronold, C. Höpfner, and H. Tributsch, Sol. Energy Mater. Sol. Cells **29**, 289 (1993).
[8] P. P. Altermatt, T. Kiesewetter, K. Ellmer, and H. Tributsch, Sol. Energy Mater. Sol. Cells **71**, 181 (2002).
[9] V. Eyert, K.-H. Höck, S. Fiechter, and H. Tributsch, Phys. Rev. B **57**, 6350 (1997).
[10] M. Birkholz, S. Fiechter, A. Hartmann, and H. Tributsch, Phys. Rev. B **43**, 11926 (1991).
[11] S. Fiechter, M. Birkholz, A. Hartmann, P. Dulski, M. Giersig, H. Tributsch, and R. J. D. Tilley, J. Mater. Res. **7**, 1829 (1992).
[12] W. Puff, M. Birkholz, A. G. Balogh, and S. Fiechter, Mater. Sci. Forum **255–257**, 342 (1997).
[13] P. J. Masset and R. A. Guidotti, J. Power Sources **177**, 595 (2008).
[14] G. Wächtershäuser, Origins Life Evol. Biosphere **20**, 173 (1990).
[15] H. Tributsch, S. Fiechter, D. Jokisch, J. Rojas-Chapana, and K. Ellmer, Origins Life Evol. Biosphere **32**, 129 (2003).
[16] R. D. Shannon and C. T. Prewitt, Acta Crystallogr. B **25**, 925 (1969).
[17] R. D. Shannon, Acta Crystallogr. A **32**, 751 (1976).
[18] M. Birkholz, Z. Phys. B **96**, 333 (1995).
[19] M. Birkholz, J. Phys.: Condens. Matter **4**, 6227 (1992).
[20] M. Birkholz, Z. Phys. B **96**, 325 (1995).
[21] M. Birkholz, Optical Absorption Coefficient of Pyrite (FeS_2), in: 11th EC Photovoltaic Solar Energy Conference, Montreux, Switzerland, 1992 (Harwood, Chur, 1993), pp. 344–347.
[22] E. D. Stevens, M. L. DeLucia, and P. Coppens, Inorg. Chem. **19**, 813 (1980).
[23] E. Nowack, D. Schwarzenbach, and T. Hahn, Acta Crystallogr. B **47**, 650 (1991).
[24] E. Nowack, D. Schwarzenbach, W. Gonschorek, and T. Hahn, Z. Kristallogr. **186**, 213 (1989).
[25] H. E. King and C. T. Prewitt, Am. Mineral. **64**, 1265 (1979).
[26] T. Chattopadhyay, H. G. von Schnering, R. F. D. Stansfield, and G. J. McIntyre, Z. Kristallogr. **199**, 13 (1992).
[27] T. A. Bither, C. T. Prewitt, J. L. Gillson, P. E. Bierstedt, R. B. Flippen, and H. S. Young, Solid State Commun. **4**, 533 (1966).
[28] T. A. Bither, R. J. Bouchard, W. H. Cloud, P. C. Donohue, and W. J. Siemons, Inorg. Chem. **7**, 2208 (1968).
[29] M. Birkholz and R. Rudert, Z. Phys. B **97**, 7 (1995).
[30] R. Tappero, I. Baraille, and A. Lichanot, Phys. Rev. B **58**, 1236 (1998).
[31] H. Ueda, M. Nohara, K. Kitazawa, H. Takagi, A. Fujimori, T. Mizokawa, and T. Yagi, Phys. Rev. B **65**, 155104 (2002).

